

Thermodynamic properties of short-range attractive Yukawa fluid: Simulation and theory

Pedro Orea

*Programa de Ingeniería Molecular, Instituto Mexicano del Petróleo,
Eje Central Lázaro Cárdenas 152, 07730 México D.F., México.*

Carlos Tapia-Medina

*Departamento de Energía, Universidad Autónoma Metropolitana-Azcapotzalco,
Av. San Pablo 180, Col. Reynosa, 02200 México D.F., México.*

Davide Pini

*Dipartimento di Fisica, Università degli Studi di Milano,
Via Celoria 16, 20133 Milano, Italy*

Albert Reiner

Erzbischöfliches Priesterseminar, Boltzmannngasse 7-9/303, A-1090 Vienna, Austria

Abstract

Coexistence properties of the hard-core attractive Yukawa potential with inverse-range parameter $\kappa = 9, 10, 12$ and 15 are calculated by applying canonical Monte Carlo simulation. As previously shown for longer ranges, we show that also for the ranges considered here the coexistence curves scaled by the critical density and temperature obey the law of corresponding states, and that a linear relationship between the critical density and the reciprocal of the critical temperature holds. The simulation results are compared with the predictions of the self-consistent Ornstein-Zernike approximation, and a good agreement is found for both the critical points and the coexistence curves, although some slight discrepancies are present.

I. INTRODUCTION

Short-range potential models of simple analytic form have been the object of intense investigation over the last years. The main reason for such an interest is that they provide an approximate representation of the effective interactions and phase behavior experimentally observed in a variety of real systems. For instance, globular protein solutions, colloidal suspensions, and fullerenes at high temperature [1–5]. This scenario has been further enriched by recent investigations of gas-solid, solid-solid, and a metastable vapor-liquid transition in one of the most studied short-range models, namely the hard-core attractive Yukawa (HCAY) potential [6–12]. The HCAY model is given by

$$u(r) = \begin{cases} \infty, & \text{if } r < \sigma, \\ -\epsilon\sigma \exp[-\kappa(r - \sigma)]/r, & \text{if } \sigma \leq r, \end{cases} \quad (1)$$

where ϵ is the depth of the potential and σ is the hard-sphere diameter. The range of the potential is tuned by varying κ . Our results are given in dimensionless units, such that $r^* = r/\sigma$ for distance, $T^* = k_B T/\epsilon$ for temperature (k_B is the Boltzmann's constant), $\rho^* = \rho\sigma^3$ for density.

Many theoretical approaches have been used for studying the HCAY fluid, for example: the Barker-Henderson perturbation theory [2, 13], the thermodynamic perturbation theory (TPT) [9, 14–17] and a variety of other mean field approaches based on truncation or approximate summation of perturbative series [18, 19], the mean spherical approximation (MSA) [10, 20–22], the modified hypernetted chain approximation (MHNC) [23] and other integral equation theories [24, 25], the density functional theory [8, 26], the self-consistent Ornstein-Zernike approximation (SCOZA) [1, 27–30], and the hierarchical reference theory (HRT) [23, 31], among others. For all theories, the most difficult regime to deal with is that of short interaction range, where an accurate localization of the vapor-liquid coexistence curve and of the critical point presents severe difficulties. Sometimes, the shape of the coexistence curve is not reproduced correctly and critical points are not located correctly either, especially the critical density. We found that the critical density data reported by these approaches show different tendencies for shorter-range attractions, when we plot ρ_c^* versus $1/T_c^*$. These issues were some of the motivations to carry out this work.

For large values of $\kappa > 7$, the computer simulation data for HCAY fluid are quite

scarce. In this regime, Gibbs ensemble Monte Carlo (GEMC) cannot reproduce binodal curves [6, 32]. The phase diagram at large κ was studied by Monte Carlo supplemented by thermodynamic integration (MC-TI) in Ref. [7], but the results do not include the critical density. In our previous works we reported the coexistence properties of HCAY fluid for long range tails. These properties were compared to those reported in the literature, and some differences were found among them [33–35]. In a recent work, Singh [36] has reported the coexistence curves of short-range attractive Yukawa (SR-HCAY) fluid with $\kappa = 8 - 10$, using Grand-canonical transition-matrix Monte Carlo (GC-TMMC) with the histogram reweighting method. However, this method proves difficult to use in order to calculate coexistence properties at low temperature and high liquid densities [36]. So, NVT-MC simulations appear to be a more efficient method to calculate such properties for very short-range systems, where these conditions are met.

In view of the above considerations, the main goals of this paper are to demonstrate that there is a linear dependence between the critical density and the reciprocal of the critical temperature even for short interaction ranges, where theoretical approaches show different tendencies, and to report a systematic study of the liquid-vapor phase diagrams of SR-HCAY fluid with $\kappa = 9, 10, 12$ and 15 , using canonical ensemble Monte Carlo simulation, where most theoretical approaches fail and other simulation techniques cannot reproduce the binodal curves. Finally, once again we have confirmed that the coexistence curves of SR-HCAY model follow the law of corresponding states, i.e., curves corresponding to different κ fall on top of each other within a high degree of accuracy, provided the density ρ and temperature T are rescaled by their critical values ρ_c, T_c .

Besides, we have also reported the binodal curves and critical points predicted by SCOZA for the above values of κ . Although the application of SCOZA to narrow Yukawa potentials has been considered before [1, 23], an extensive comparison with simulation data for the phase diagram in this regime has not been possible so far because of the aforementioned paucity of simulations at large κ , and the present study represents a good opportunity to perform it. Results were obtained both by the standard version of SCOZA considered in Refs. [1, 23, 28], and by a modified version developed in [29], where consistency with the virial route, which is disregarded in the original implementation, is partially taken into account. The comparison shows that some discrepancies between SCOZA and simulations are definitely present: specifically, the standard formulation of SCOZA overestimates both

the critical density and critical temperature, while the converse happens with the modified formulation. The latter also predicts a nearly constant critical density at values of κ , for which the simulation show that this quantity still changes significantly. Nevertheless, the overall agreement with the simulations is quite satisfactory.

The paper is organized as follows: in Sec. II the details of our simulations are briefly summarized; in Sec. III, an overview of both the standard and the modified versions of SCOZA is given, and some issues relevant for the application of the theory to short-range interactions are discussed; in Sec. IV our results are presented and discussed; in Sec. V our conclusions are drawn.

II. SIMULATION DETAILS

Canonical ensemble Monte Carlo (NVT-MC) simulations of HCAY fluid interface have been performed using Metropolis algorithm. To prepare the initial configuration we placed $N = 1726$ particles in a face-centered cubic array in the middle of the simulation cell, which allowed us to obtain two interfaces with a vapor phase surrounding the liquid when the system is equilibrated (see Fig 2 of Ref.[33]).

Simulations were performed on a parallelepiped cell with dimensions $L_x = L_y = 10$, and $L_z = 40$. Additional MC runs were carried out with $L_x = L_y = 14$ and a larger number of particles [37, 38] to check for finite-size effects, and no such effect was found. The cutoff radius was selected to $R_c = 2$. Periodic boundary conditions were applied in all three directions and the neighbor list was applied to speed up calculation. The maximum particle displacement was adjusted to give a 45% acceptance rate. The simulations were performed in cycles; in every cycle it was attempted to move all the particles that are in the neighbor list. The system was equilibrated for 10^6 cycles and the coexistence properties were calculated for 10^7 cycles divided into 100 blocks of 10^5 cycles each one, in order to avoid density fluctuation.

The density profiles, $\rho(z)$, were calculated every 50 cycles and at the end of each simulation run, every profile was fitted to a hyperbolic tangent function to obtain ρ_V^* and ρ_L^* values[33–35]. The critical parameters for the HCAY fluid were calculated by using the rectilinear diameter law [39] and the universal value $\beta_{coex} = 0.325$ for the critical exponent

β_{coex} which gives the curvature of the liquid-vapor coexistence curve in the critical region. All the critical point parameters we calculated are listed in Table I.

III. THEORY

A detailed description of SCOZA and its application to a Yukawa fluid has been given elsewhere and we refer the interested reader to the previous literature on this subject [1, 23, 27, 28]. Here we recall that, as usual in integral-equation theories, in the SCOZA the Ornstein-Zernike (OZ) equation is closed by an approximate *ansatz* which involves the direct correlation function $c(r)$ and the radial distribution function $g(r)$. In the standard formulation of SCOZA, one requires that i) the core condition $g(r) = 0$ be satisfied inside the hard core $r < \sigma$; and ii) the contribution to $c(r)$ outside the hard core due to tail of the potential be linear in the potential itself. For a HCAY potential one has then:

$$\begin{cases} g(r) = 0 & \text{if } r < \sigma, \\ c(r) = c_{HS}(r) + K \exp[-\kappa(r - \sigma)]/r & \text{if } \sigma \leq r, \end{cases} \quad (2)$$

where $c_{HS}(r)$ is the direct correlation function of the hard-sphere fluid. The functional form of this closure is similar to that of well-established theories such as the mean spherical approximation (MSA), where $c_{HS}(r)$ is identically vanishing for $r > \sigma$, or the optimized random-phase approximation (ORPA) [40]. However, in these approaches the amplitude K of the direct correlation function coincides with the inverse temperature $\beta = 1/(k_B T)$, while in the SCOZA K is an *a priori* unknown function of the thermodynamic state, to be determined so that consistency between the compressibility and the internal energy route to the thermodynamic is obtained. The consistency requirement is embodied in the following condition on the reduced compressibility χ_{red} and the excess internal energy per unit volume u :

$$\frac{\partial}{\partial \beta} \left(\frac{1}{\chi_{red}} \right) = \rho \frac{\partial^2 u}{\partial \rho^2}, \quad (3)$$

where χ_{red} and u are obtained via the compressibility and internal energy route respectively. Eq. (3) together with closure (2) give a closed partial differential equation (PDE) for u , that can be solved numerically, provided the initial condition at $\beta = 0$ and the boundary conditions at low and high density are specified. The solution procedure is made easier by the fact that, for a given K , the OZ equation with closure (2) can be solved analytically,

if $c(r)$ for $r > \sigma$ is given by a superposition of Yukawa tails [41]. This is indeed the case, provided one adopts the Waisman parametrization for the hard-sphere direct correlation function $c_{HS}(r)$ [42]. According to this, $c_{HS}(r)$ for $r > \sigma$ is also given by a Yukawa tail with known, density-dependent amplitude and range, so that $c(r)$ for $r > \sigma$ consists of the superposition of two Yukawas. On the other hand, for non-Yukawa intermolecular potentials the SCOZA $c(r)$ for $\sigma \leq r$ is not of Yukawa form, irrespective of the parametrization adopted for $c_{HS}(r)$, and in order to implement SCOZA a fully numerical solution of the OZ equation is usually required [43, 44].

In conventional SCOZA, the virial route is not included in the consistency condition. In order to enforce consistency among all the three routes, one has to endow Eq. (2) with one more degree of freedom. To this purpose, the following form for $c(r)$ was proposed [29]:

$$c(r) = c_{HS}(r) + \beta \exp[-\kappa(r - \sigma)]/r + H \exp[-z(r - \sigma)]/r \quad \text{if } \sigma \leq r, \quad (4)$$

where the amplitude of the (attractive) Yukawa potential has now been set to β as in the MSA, while both the amplitude H and the inverse range z of the extra Yukawa tail must be determined by imposing consistency among virial, compressibility, and internal energy. This approach is very similar to that originally proposed in Ref. [45], which is obtained from Eq. (4) by having the last Yukawa to account also for the hard-sphere contribution to $c(r)$ outside the repulsive core, thereby setting $c_{HS}(r) = 0$ in Eq. (4). A fully numerical implementation of that closure was considered in Ref. [23], but the numerical algorithm failed to converge in the critical region. In a recent work [29], a different strategy was adopted: on the one hand, the analytical solution of the OZ equation for a $c(r)$ given by a superposition of Yukawas (three when also $c_{HS}(r)$ is taken into account) for $\sigma \leq r$ was again exploited. On the other hand, consistency with the virial route was required to hold only at the critical point, and z was fixed at the value at which this condition is satisfied, thereby making the theory considerably easier to implement. This is the approach used here together with the standard SCOZA of Eqs. (2), (3). In the following the standard and modified versions of SCOZA will be referred to as S-SCOZA and M-SCOZA respectively.

Before concluding this Section, it is worthwhile adding some remarks about the relevance of the high-density boundary condition for the SCOZA PDE. While the boundary condition at low density is trivial, since one must have $\chi_{red}(\rho=0, \beta) = 1$, $u(\rho=0, \beta) = 0$ for every β ,

the behavior at high density poses more problems. In fact, this is not known beforehand, so that there is a certain amount of arbitrariness on the form of the corresponding boundary condition. For instance, in Refs. [1, 23, 28], the boundary condition was imposed on $\partial^2 u / \partial \rho^2$, which was set to the value obtained by the so-called high-temperature approximation (HTA) [40], i.e., by replacing u with its zeroth-order contribution in an expansion in powers of β . In Ref. [29], instead, the boundary condition was imposed directly on u rather than on its derivative, and u was determined using the $g(r)$ obtained via the ORPA, which amounts to setting $K = \beta$ in Eq. (2). Since there is not any obvious recipe for singling out a specific high-density boundary condition, a natural requirement is that the results should not depend on the detailed form of such a condition, or on the density ρ_0 at which it is imposed. This turns out to be indeed the case, provided ρ_0 is high enough. For Lennard-Jones like tails, such as that corresponding to the widely adopted value $z = 1.8$ [28], setting the high-density boundary at $\rho_0^* = 1$ proves to be amply sufficient. However, for interactions of shorter range, such as those considered in Ref. [1] as well as in the present paper, ρ_0 must be shifted to substantially higher densities. This was also observed in a fully numerical implementation of SCOZA for a square-well fluid [43]. In fact, for the largest value of z considered here, $z = 25$ (see Table I), ρ_0 must be at least as high as the close-packing density $\rho_0^* = \sqrt{2}$, and at even larger z one needs to move ρ_0 beyond close packing. This requirement sounds quite unphysical, but one should keep in mind that here the effect of the singular repulsion is described at the level of the Carnahan-Starling equation of state [40], which is itself unaware of close packing, and has the compressibility vanish at the unphysical value $\rho^* = 6/\pi$ rather than at $\rho^* = \sqrt{2}$. The HTA for u is expected to become exact at close packing [46], but in view of the above, it is not surprising that one might need to go beyond close packing for the hard-sphere repulsion to overwhelm the attractive part of the interaction in $g(r)$.

If the boundary is not located at sufficiently high ρ_0 , the results turn out to be very sensitive with respect to both a shift in ρ_0 , and the details of the boundary condition. This observation is relevant for some of the results reported in Ref. [29], where both S-SCOZA and M-SCOZA calculations were performed for different values of z , but the high-density boundary was always kept fixed at $\rho_0^* = 1$. This is adequate for $z \lesssim 8$, but for larger z it leads to an underestimation of both the critical density and the critical temperature with respect to the genuine SCOZA result, which becomes more and more severe as z is increased. The results presented here are not affected by this spurious effect, and are meant to supersede

those shown in Table I of Ref. [29].

IV. RESULTS AND DISCUSSIONS

We start our discussion with an analysis of the critical values of HCAY fluid. Table I presents the reduced critical temperature T_c^* and density ρ_c^* for a wide range of κ predicted by both simulations and several theoretical approaches, namely, the S-SCOZA and M-SCOZA described in the previous section, the TPT by Zhou [14], and the equation of state (EOS) by Duh and Mier-Y-Teran [22]. We recall that, as λ is increased, the liquid-vapor critical point becomes metastable with respect to freezing. According to many theoretical and simulation studies [1, 6–8, 10, 11], for $\lambda \geq 7$ the metastable regime has already set in.

κ	T_c^*	ρ_c^*	Method	Ref.
1.8	1.180	0.313	NVT-MC	[34]
1.8	1.180	0.315	GC-TMMC	[36]
1.8	1.212	0.312	GC-FSS ^a	[28]
1.8	1.219	0.314	S-SCOZA	[28]
1.8	1.246	0.310	TPT	[14]
1.8	1.240	0.318	MSA-EOS	[22]
2.0	1.050	0.322	NVT-MC	[34]
2.0	1.088	0.323	S-SCOZA	this work
2.5	0.840	0.336	NVT-MC	[34]
2.5	0.871	0.342	S-SCOZA	this work
3.0	0.721	0.356	NVT-MC	[34]
3.0	0.722	0.355	GC-TMMC	[36]
3.0	0.740	0.359	S-SCOZA	this work
3.0	0.764	0.379	MSA-EOS	[22]
4.0	0.581	0.380	NVT-MC	[33]
4.0	0.572	0.385	GC-TMMC	[36]
4.0	0.591	0.389	S-SCOZA	[23]
4.0	0.579	0.375	M-SCOZA	this work
4.0	0.588	0.414	TPT	[14]

4.0	0.614	0.428	MSA-EOS	[22]
5.0	0.500	0.39	NVT-MC	[33]
5.0	0.509	0.416	S-SCOZA	this work ^b
5.0	0.497	0.393	M-SCOZA	this work
5.0	0.530	0.472	MSA-EOS	[22]
6.0	0.448	0.412	NVT-MC	[33]
6.0	0.456	0.438	S-SCOZA	this work ^b
6.0	0.445	0.407	M-SCOZA	this work
7.0	0.414	0.422	NVT-MC	[33]
7.0	0.419	0.457	S-SCOZA	[23]
7.0	0.409	0.418	M-SCOZA	this work
7.0	0.411	0.502	TPT	[14]
8.0	0.382	0.447	GC-TMMC	[36]
8.0	0.392	0.474	S-SCOZA	this work
8.0	0.383	0.426	M-SCOZA	this work
9.0	0.365	0.456	NVT-MC	this work
9.0	0.362	0.454	GC-TMMC	[36]
9.0	0.370	0.489	S-SCOZA	this work
9.0	0.368	0.433	M-SCOZA	this work
10.0	0.347	0.466	NVT-MC	this work
10.0	0.343	0.471	GC-TMMC	[36]
10.0	0.352	0.503	S-SCOZA	this work
10.0	0.345	0.439	M-SCOZA	this work
10.0	0.361	0.652	MSA-EOS	[22]
11.0	0.337	0.515	S-SCOZA	this work
11.0	0.331	0.444	M-SCOZA	this work
12.0	0.323	0.480	NVT-MC	this work
12.0	0.324	0.525	S-SCOZA	this work
12.0	0.319	0.447	M-SCOZA	this work
15.0	0.292	0.515	NVT-MC	this work

15.0	0.293	0.551	S-SCOZA	this work
15.0	0.291	0.455	M-SCOZA	this work
25.0	0.235	0.555	MC-TI	[7] ^c
25.0	0.236	0.600	S-SCOZA	this work
25.0	0.241	0.459	M-SCOZA	this work
25.0	0.239	0.632	TPT	[14]

TABLE I: Critical parameters of HCAY Fluid.

^aGran canonical Monte Carlo with finite-size scaling.

^bThe calculation for this value of κ had already been performed in Ref. [1], but the result had not been tabulated.

^c ρ_c was obtained using Eq. (4) from Ref. [35].

The critical density as a function of the inverse of the critical temperature as obtained from our simulations and the aforementioned theories is shown in Fig. 1. The critical simulation data obtained by Singh using GC-TMMC, also displayed in the figure, are in excellent agreement with ours, which shows that both techniques give similar results within the error bar. At small κ , all theories give similar results, and are in good agreement with the simulations. In fact, in the long-range regime even a simple mean-field approach along the lines of the van der Waals theory provides an accurate description of the system, which has been shown to become exact in the limit where the range of the tail potential goes to infinity, and its strength goes to zero [47]. As the interaction range gets shorter, discrepancies become more and more pronounced, especially as far as ρ_c^* is concerned. In particular, the data for ρ_c^* reported by Duh and Mier-Y-Teran [22] using their equation of state (EOS) for HCAY fluid strongly overestimate the simulations. The TPT by Zhou [14] and the S-SCOZA show a better agreement with the simulation data. The latter are bracketed by the S-SCOZA and M-SCOZA results: S-SCOZA overestimates both ρ_c^* and T_c^* , while the converse is true for M-SCOZA. For both approaches, the relative error with respect to the simulations is in general considerably smaller for T_c^* than for ρ_c^* .

The most remarkable feature of the simulation results is the linear trend for ρ_c^* vs. $1/T_c^*$ up to inverse-range parameters as large as $\kappa = 15$, corresponding to $1/T_c^* = 3.425$. A similar behavior is displayed by S-SCOZA, as well as by TPT. As κ is further increased, the slopes

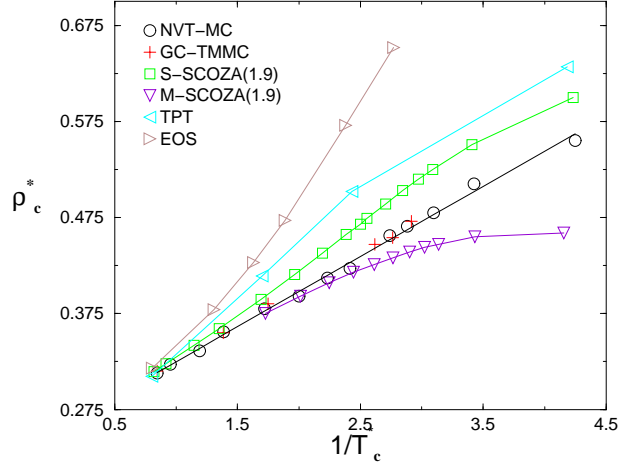


FIG. 1: Relation between critical density and inverse critical temperature of HCAY model for different simulation and theoretical results. NVT-MC with $1.8 \leq \kappa \leq 15$ from this and previous works [33–35]. GC-TMMC with $1.8 \leq \kappa \leq 10$ [36]. SCOZA with $1.8 \leq \kappa \leq 25$ from this and previous works [1, 23, 28], M-SCOZA with $4 \leq \kappa \leq 25$ from this work, EOS with $1.8 \leq \kappa \leq 12$ [22], and TPT with $1.8 \leq \kappa \leq 25$ [14].

of both SCOZA and TPT plots start to decrease, and deviations from linearity become apparent. This is consistent with the fact that, as the potential range goes to zero and $1/T_c^*$ diverges, one expects ρ_c^* to tend to a finite, non-vanishing value. Such a qualitative behavior is predicted by Baxter’s analytical solution of his adhesive hard-sphere (AHS) model [48], and has recently been supported by MC simulations of the AHS model itself [49, 50] as well as of square-well fluids with very short attraction range [51]. It may also be recalled that for the HCAY fluid, a finite value of ρ_c^* in the limit of vanishing attraction range is found analytically also within MSA [52]. We did not perform simulations for $\kappa > 15$, but we took the critical temperature for $\kappa = 25$ obtained in Ref. [7], and inserted it into Eq. (4) of Ref. [35] to obtain the critical density. The result, also plotted in Fig. 1, shows a trend similar to that of S-SCOZA. In this respect, it may be observed that, although M-SCOZA has the best agreement with simulations for $\kappa < 15$, it overemphasizes the tendency to saturation at larger κ [53], which is better described by S-SCOZA.

We now turn to the dependence of the critical temperature on the interaction range. For hard-core plus attractive tail potentials, it has been suggested that the second virial coefficient at the critical temperature $B_2(T_c)$ has a practically constant value B_2^c , and that

short-range tails follow a universal behavior, provided the second virial coefficient $B_2(T)$ is used as the temperature-like variable instead of the temperature itself [54, 55]. Specifically, it should be possible to map the system into a hard-core plus square-well fluid with the same hard-core diameter, and a temperature-dependent range δ determined so as to give the same B_2 at the same reduced temperature T^* as those of the original interaction. As a consequence, for small enough ranges the reduced critical temperature should fulfill the relation

$$\frac{1}{T_c^*} = \ln \left[1 + \frac{1 - B_2^c/B_2^{HS}}{(1 + \delta)^3 - 1} \right], \quad (5)$$

where B_2^{HS} is the virial coefficient of the hard-sphere fluid. Subsequent work [8, 35, 56, 57] has shown that, even for short-range interactions, $B_2(T_c)$ changes systematically with the attraction range. Nevertheless, at short range Eq. (5) does represent quite accurately our results for T_c^* . This is shown in Fig. 2, where T_c^* as predicted by both simulations and theories has been plotted as a function of the effective square-well range δ , and compared with Eq. (5) by taking B_2^c as a fitting parameter. It can be noticed that all the theories considered here agree reasonably well with the simulations, and the discrepancies are smaller than those found for ρ_c^* . Moreover, for $\delta \lesssim 0.2$, T_c^* is indeed well represented by Eq. (5) with $B_2^c/B_2^{HS} \simeq -1.35$. In fact, at short range the effective range δ is much less sensitive than $B_2(T)$ to small changes in temperature, so that Eq. (5) can be satisfied to a very good degree, even though $B_2(T_c)$ is not actually constant.

If $B_2(T_c)$ tends to a finite limit B_2^{AHS} for $\delta \rightarrow 0$, Eq. (5) with $B_2^c = B_2^{AHS}$ will hold for potentials of arbitrarily short range down to the AHS limit. Such a behavior was found by Largo et al. [51] for the square-well fluid. We are not able to state if this is the case also for the Yukawa fluid since, for the interval of κ considered in this work, our simulation results do not provide a clear evidence of $B_2(T_c)$ saturating to a finite limit. In this respect, we should notice that the value $B_2^c/B_2^{HS} \simeq -1.35$ found here is lower than both the result of Largo et al. [51] $B_2^c/B_2^{HS} = -1.174$ and that of Miller and Frenkel [49] $B_2^c/B_2^{HS} = -1.21$.

Our new phase equilibrium data of HCAY fluid with $\kappa = 9, 10, 12$, and 15 are shown in Fig. 3, and compared to those reported by Singh [36] for $\kappa = 9$ and $\kappa = 10$. An excellent agreement is found between them. Therefore, both simulation techniques are good for calculating such properties. It is worth noting that the NVT-MC technique is more efficient for the calculation of the coexistence properties of very short-range systems and

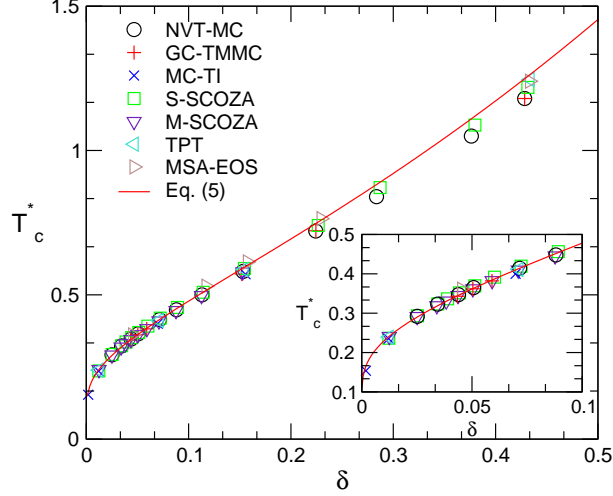


FIG. 2: Relation between critical temperature and effective range δ (see text) of the HCAY model for different simulation and theoretical results. Symbols have the same meaning as in Fig. 1. MC-TI with $3.9 \leq \kappa \leq 100$ from Ref. [7]. The red line represents the prediction of Eq. (5). The inset is an enlargement of the short-range region.

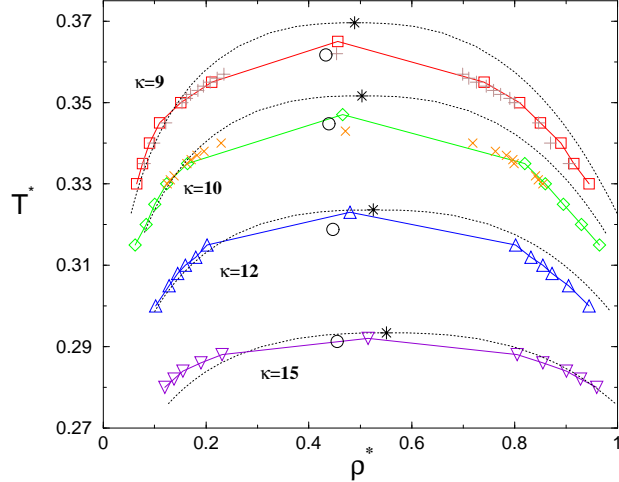


FIG. 3: Vapor-liquid coexistence curves of SR-HCAY fluid. Open symbols are NVT-MC data from this work. Other symbols are GC-TMMC data from Ref. [36]. Dotted lines are S-SCOZA results from this work. Starbursts and circles are S-SCOZA and M-SCOZA critical points, respectively.

at low temperature, where other simulation techniques such as GEMC or GC-TMMC run into considerable difficulties, because the high liquid density of the systems makes particle insertion very time-consuming. Our simulation results for the coexistence curve are reported in Table II. Figure 3 also shows the coexistence curves and the critical points predicted

κ	T^*	ρ_L	ρ_V
9.0	0.330	0.945	0.0650
	0.335	0.915	0.0766
	0.340	0.890	0.0900
	0.345	0.850	0.1100
	0.350	0.810	0.1510
	0.355	0.741	0.2110
10.0	0.315	0.965	0.0621
	0.320	0.930	0.0834
	0.325	0.895	0.1005
	0.330	0.860	0.1233
	0.335	0.820	0.1638
12.0	0.300	0.945	0.1021
	0.305	0.905	0.1282
	0.308	0.873	0.1454
	0.310	0.855	0.1603
	0.312	0.832	0.1802
	0.315	0.802	0.2022
15.0	0.280	0.960	0.1201
	0.282	0.928	0.1380
	0.284	0.901	0.1550
	0.286	0.855	0.1900
	0.288	0.805	0.2310

TABLE II: Coexistence properties of SR-HCAY fluid at different interaction ranges.

by S-SCOZA, and the M-SCOZA critical points. M-SCOZA coexistence curves have not been reported, because we could not rule out the possibility that they may be affected by significant numerical errors. It appears that the main source of discrepancy between the simulation and theoretical phase diagrams lies in the position of the critical points whose densities and temperatures, as observed above, are both slightly overestimated by S-SCOZA. Figure 4 shows the reduced density as a function of the reduced temperature. All curves of

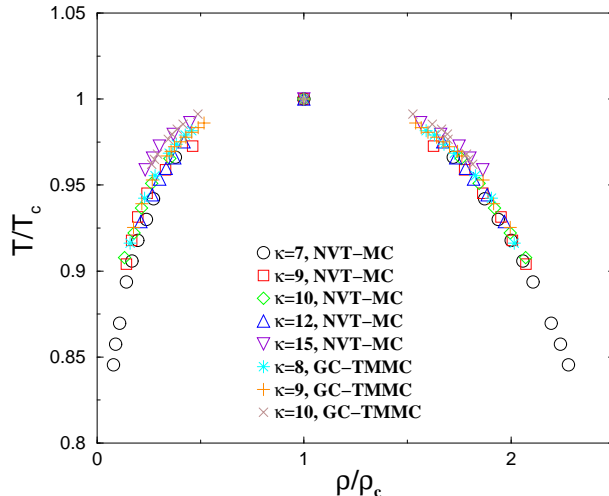


FIG. 4: Reduced vapor-liquid coexistence curves of SR-HCAY fluid. NVT-MC data from this work and Ref. [33]. GC-TMMC data from Ref. [36].

short range HCAY fluid form a single master curve within a very good degree of accuracy, as it was reported by one of us in a previous work for longer range [35]. As the range is decreased, a slight trend towards a widening of the coexistence curve can be detected, but this effect remains small for the ranges considered here. Also, the coexistence curves reported by Singh [36] using GC-TMMC are on the master curve. The same behavior has been found for the Mie(n,m) potential [58–60]. These results confirm that, even for the short range interactions considered here, with inverse-range parameter as large as $\kappa = 15$, the vapor-liquid phase diagrams of HCAY fluid obey the law of corresponding states. This fact could be used to test theoretical approaches.

V. CONCLUSIONS

We have carried out a systematic study of the liquid-vapor phase diagrams for hard-core attractive Yukawa potential with $\kappa = 9, 10, 12$ and 15 , using NVT-MC simulation. Our coexistence curves for $\kappa = 9$ and 10 were compared to those reported by Singh using GC-TMMC. An excellent agreement was found between them. Besides, we have shown that reduced coexistence curves of HCAY fluid from $\kappa = 7$ to $\kappa = 15$ follow the law of corresponding states, as it was shown in a previous work [35] for longer interaction ranges. Once again, we have confirmed the linear relationship between the critical density and inverse

critical temperature for critical simulation data in this interval of κ . The simulation results were compared with several theories, including the standard formulation of SCOZA (S-SCOZA) as well as a modified version (M-SCOZA) implementing a partial consistency with the virial route, which is disregarded in the standard version. The comparison shows that S-SCOZA slightly overestimates both the critical temperature and the critical density with respect to the simulation results, while the converse is true for M-SCOZA. Nevertheless, the agreement with the simulations is quite good for all the values of κ considered in this paper. Both simulation and theory give a dependence of the critical temperature as a function of the interaction range in substantial agreement with Noro-Frenkel scaling. However, whether the second virial coefficient at the critical temperature $B_2(T_c)$ tends to a constant as κ diverges, thereby making Noro-Frenkel scaling hold at arbitrarily short range as in the square-well case [51], could not be established on the basis of our simulation data, and remains to be assessed.

VI. ACKNOWLEDGMENTS

PO gratefully acknowledges the financial support of the Instituto Mexicano del Petróleo, under the project D.00476. DP thanks Alberto Parola, Luciano Reatto and Johan Høye for insightful conversation.

-
- [1] G. Foffi, G. D. McCullagh, A. Lawlor, E. Zaccarelli, K. A. Dawson, F. Sciortino, P. Tartaglia, D. Pini, and G. Stell, *Phys. Rev. E* **65**, 031407 (2002).
 - [2] F. W. Tavares, and J. M. Prausnitz, *Colloid Polym. Sci.* **282**, 620 (2004).
 - [3] C. Caccamo, G. Pellicane, and D. Costa, *J. Phys. : Condens. Matter* **12**, A437 (2000).
 - [4] D. F. Rosenbaum, A. Kulkarni, S. Ramakrishnan, and C. F. Zukoskia, *J. Chem. Phys.* **111**, 9882 (1999).
 - [5] J. Bergenholtz and M. Fuchs, *Phys. Rev. E* **59**, 5706 (1999); *J. Phys. : Condens. Matter* **11**, 10171 (1999).
 - [6] M. H. J. Hagen and D. Frenkel, *J. Chem. Phys.* **101**, 4093 (1994).
 - [7] M. Dijkstra, *Phys. Rev. E* **66**, 021402 (2002).

- [8] D. Fu, Y. Li, and J. Wu, Phys. Rev. E **68**, 011403 (2003).
- [9] S. Zhou, J. Phys. Chem. B **108**, 8447 (2004).
- [10] R. Tuinier , and G. J. Fleer, J. Phys. Chem. B **110**, 20540 (2006).
- [11] P. Charbonneau, and D. R. Reichman, Phys. Rev. E **75**, 011507 (2007).
- [12] Ph. Germain and S. Amokrane, Phys. Rev. E **76**, 031401 (2007).
- [13] P. Paricaud, J. Chem. Phys. **124**, 154505 (2006).
- [14] S. Zhou, Phys. Rev. E **79**, 011126 (2009); J. Chem. Phys. **130**, 054103 (2009); J. Phys. Chem. B **113**, 8635 (2009).
- [15] M. Robles and M. Lopez de Haro, J. Phys. Chem. C **111**, 15957 (2007).
- [16] R. Melnyka, I. Nezbedab, D. Hendersonc, A. Trokhymchuka, Fluid Phase Equilib. **279**, 1 (2009).
- [17] D. J. Naresh and J. K. Singh, Fluid Phase Equilib. **285**, 36 (2009).
- [18] V. C. Weiss and W. Schröer, Int. J. Thermophysics **28**, 506 (2007); J. Stat. Mech: Theory and Exp., P04020 (2008).
- [19] V. C. Weiss, Fluid Phase Equilib. **286**, 62 (2009).
- [20] D. Henderson, L. Blum, and J. P. Noworyta, J. Chem. Phys. **102**, 4973 (1995).
- [21] J. H. Herrera, H. Ruiz-Estrada and L. Blum, J. Chem. Phys. **104**, 6327 (1996).
- [22] D.-M. Duh and L. Mier-Y-Terán, Mol. Phys. **90**, 373 (1997).
- [23] C. Caccamo, G. Pellicane, D. Costa, D. Pini, and G. Stell, Phys. Rev. E **60**, 5533 (1999).
- [24] E. B. El Mendoub, J. F. Wax, and N. Jakse, Phys. Rev. E **74**, 052501 (2006).
- [25] A. Ayadim, M. Oettel, and S. Amokrane, J. Phys.: Condens. Matter **21**, 115103 (2009).
- [26] D. Fu, and J. Wu, Mol. Phys. **102**, 1479 (2004).
- [27] D. Pini, G. Stell, and J. S. Høye, Int. J. Thermophys. **19**, 1029 (1998).
- [28] D. Pini, G. Stell, and N. B. Wilding, Mol. Phys. **95**, 483 (1998).
- [29] A. Reiner and J. S. Hoye, J. Chem. Phys. **128**, 114507 (2008).
- [30] J-M Caillol, F. Lo Verso, E. Scholl-Paschinger, and J-J Weis, Mol. Phys. **105**, 1813 (2007) .
- [31] A. Parola, D. Pini, and L. Reatto, Phys. Rev. Lett. **100**, 115103 (2008); Mol. Phys. **107**, 503 (2009).
- [32] E. Lomba and N. G. Almarza, J. Chem. Phys. **100**, 8367 (1994).
- [33] Y. Duda, A. Romero-Martinez, and P. Orea, J. Chem. Phys. **126**, 224510 (2007).
- [34] U. F. Galicia-Pimentel, J. López-Lemus, and P. Orea, Fluid Phase Equilib. **265**, 205 (2008).

- [35] P. Orea and Y. Duda, *J. Chem. Phys.* **128**, 134508 (2008).
- [36] J. K. Singh, *Mol. Sim.* **35**, 880 (2009).
- [37] P. Orea, J. López-Lemus, and J. Alejandre, *J. Chem. Phys.* **123**, 114702 (2005).
- [38] F. Biscay, A. Ghoufi, F. Goujon, V. Lachet, and P. Malfreyt, *J. Chem. Phys.* **130**, 184710 (2009).
- [39] D. P. Landau, K. Binder, *A guide to Monte Carlo simulations in statistical physics*, (Cambridge University Press, Cambridge, 2000).
- [40] J. P. Hansen and I. R. McDonald, *Theory of Simple Liquids*, 3rd ed. (Academic Press, London, 2006).
- [41] J. S. Høye, G. Stell, and E. Waisman, *Mol. Phys.* **32**, 209 (1976); J. S. Høye and L. Blum, *J. Stat. Phys.* **16**, 399 (1977).
- [42] E. Waisman, *Mol. Phys.* **25**, 45 (1973).
- [43] E. Schöll-Paschinger, A. L. Benavides, and R. Castañeda-Priego, *J. Chem. Phys.* **123**, 234513 (2005).
- [44] F. F. Betancourt-Cardenas, L. A. Galicia-Luna, A. L. Benavides, J. A. Ramirez, and E. Schöll-Paschinger, *Mol. Phys.* **106**, 113 (2008).
- [45] J. S. Høye and G. Stell, *Mol. Phys.* **52**, 1071 (1984).
- [46] G. Stell and O. Penrose, *Phys. Rev. Lett.* **51**, 1397 (1983).
- [47] M. Kac, G. E. Uhlenbeck, and P. C. Hemmer, *J. Math. Phys.* **4**, 216 (1963); N. G. van Kampen, *Phys. Rev.* **135**, 362 (1964); J. L. Lebowitz and O. Penrose, *J. Math. Phys.* **7**, 98 (1966).
- [48] R. J. Baxter, *J. Chem. Phys.* **49**, 2770 (1968).
- [49] M. A. Miller and D. Frenkel, *Phys. Rev. Lett.* **90**, 135072 (2003).
- [50] M. A. Miller and D. Frenkel, *J. Phys.: Condens. Matter* **16**, S4901 (2004).
- [51] J. Largo, M. A. Miller, and F. Sciortino, *J. Chem. Phys.* **128**, 134513 (2008).
- [52] L. Mier-Y-Terán, E. Corvera, and A. E. Gonzáles, *Phys. Rev. A* **39**, 371 (1989).
- [53] In fact, in Ref. [29] S-SCOZA was mainly intended for Lennard-Jones like potentials.
- [54] G. A. Vliegthart and H. N. W. Lekkerkerker, *J. Chem. Phys.* **112**, 5364 (2000).
- [55] M. G. Noro and D. Frenkel, *J. Chem. Phys.* **113**, 2941 (2000).
- [56] R. López-Rendón, Y. Reyes, and P. Orea, *J. Chem. Phys.* **125**, 084508 (2006).
- [57] S. Zhou, *Mol. Sim.* **33**, 1187 (2007).

- [58] H. Okumura and F. Yonezawa, *J. Chem. Phys.* **113**, 9162 (2000).
- [59] P. Orea, Y. Reyes-Mercado, and Y. Duda, *Phys. Lett. A* **372**, 7024 (2008).
- [60] G. Galliero, M. M. Piñeiro, B. Mendiboure, C. Miqueu, T. Lafitte, and D. Bessieres, *J. Chem. Phys.* **130**, 104704 (2009).